Preprints.org

Article

Modular UV Curing Sol-Gel Coating for Invisible, Levelling and Easy to Clean Multi-Layer Systems.

Lucía Florentino Rico * , Olga Conejero Iglesias , Ramón Bernardo De la Rua García , Jennifer Moriones Domeño , Jonathan Fernández de Ara , Gonzalo Garcia Fuentes

Article

Modular UV Curing Sol-Gel Coating for Invisible, Levelling and Easy to Clean Multi-Layer Systems

Lucía Florentino Rico [1],*, Olga Conejero Iglesias [1], Ramón Bernardo de la Rua García [1], Jennifer Moriones Domeño [2], Jonathan Fernández de Ara [2] and Gonzalo G. Fuentes [2]

[1]   Idonial Foundation, C/ Calafates, 33417 Avilés, Spain; lucia.florentino@idonial.com
[2]   AIN, Carretera Pamplona, 1. 31191 Cordovilla, Spain; jfernandez@ain.es
*   Correspondence: lucia.florentino@idonial.com

Abstract: Current methods for the hardening step of functional coatings over different materials imply the use of high temperatures, high energy consumption or long periods of time, which have repercussions on the speed and cost of the product. We report here a simple and low cost methodology for the functionalization of low cost stainless steel, which is modular, depending of the functionality pursued: a levelling layer for smooth the surface of the material, an "easy to clean" property, or both of them. The research is based on sol-gel coatings cured under UV light without requiring high thermal hardening processes making it applicable to plastics and other sensible materials and possessing high chemical and thermal stability. The film ensures lower processing costs, and higher rates of hardening if the adequate medium-pressure lamps are employed. This formulation is also well defined for scaling up the process, so it is possible to perform a continuous coating in large areas by employing mild processing conditions (low temperature, atmospheric pressure). In addition, the sol gel solution was fully characterized and studied in order to guarantee a long service life before deposition, with a focus on industrial applications in the domestic sector.

Keywords: sol-gel; UV curing; fotocurable; coating; hydrophobic; easy to clean; contact angle; levelling

1. Introduction

Sol-gel technology has been widely used since 1980 in the history of materials science [1,2] in the process of synthesizing superconducting materials [3], functional ceramic materials [4], nonlinear optical materials [5], catalysts and enzyme carriers for biomedical applications [6,7], porous glass and other materials [8,9]. This method for the developing of functional surfaces over multiple substrates is gaining much more attention since many applications are finding a reduction in cost and complexity compared with other methodologies. Among the substrates where these coatings can currently be applied there is a large repertoire, from fabrics for many textile applications [10] to polymers for conferring flame retardant features [11] or glass for the study of antifouling coatings for marine applications [12].

Sol gel SiO_2 coatings are obtained mainly by dissolving an alkoxide precursor in alcohol together with the appropriate additives, which are then hydrolyzed in water in the presence of an acid or basic catalyst source. Once the hydrosilylation reaction takes place, the alcohol molecules are condensed forming a cross-linked polysiloxane network, and at this point, the gelation process starts. After the deposition process of the solution prepared by spinning, dipping or spraying (among others) over the substrate, it is necessary to carry out a densification of the layer to complete the gelification process by heating at high temperatures or by polymerization under UV light (technology considered in this work), leading to a compact layer free of cracks or striations, chemically and physically resistant (Figure 1).

Research of sol gel coatings cured under UV light without requiring high-temperature hardening processes on plastic surfaces have recently been the center of attention. In addition to the low temperature curing process, the UV-cured films have various advantages such as high chemical and thermal stability, less harm for the environment, lower processing costs, and higher rates of hardening if the appropriate medium-pressure lamps are employed.

A photopolymerisable coating formulation essentially consists of adding a polymerisable molecule (oligomer, in the present work dipentaerythritol penta-/hexa-acrylate_ DPHA) and a light-sensitive compound or photoinitiator that is able to convert the absorbed light energy into a more useful form capable of causing the binder to polymerise into a hard solid film. The photoinitiator produces initiator radicals directly by the fragmentation of the photo-excited state, and for this kind of coatings, aromatic α-hydroxiketones like 1-hydroxycyclohexyl phenyl ketone (Irgacure 184) or 2-Hydroxy-2-methylpropiophenone (Darocure 1173) were suitable candidates [13]. In these systems, photoinitiators mainly affect cure speed, yellowing, and cost. In addition, the light absorption properties of the selected photoinitiator need to match the emission wavelength of the light source [14]. Figure 1 represents the general process for this technology, where it is noticeable how the double bonds of the acrylate molecules are eliminated upon radical reactions and co-polymerization of the different chemicals involved in the process (3-(Trimethoxysilyl) propyl methacrylate_MEMO and the acrylic monomer DPHA) causing the total gelification of the coating.
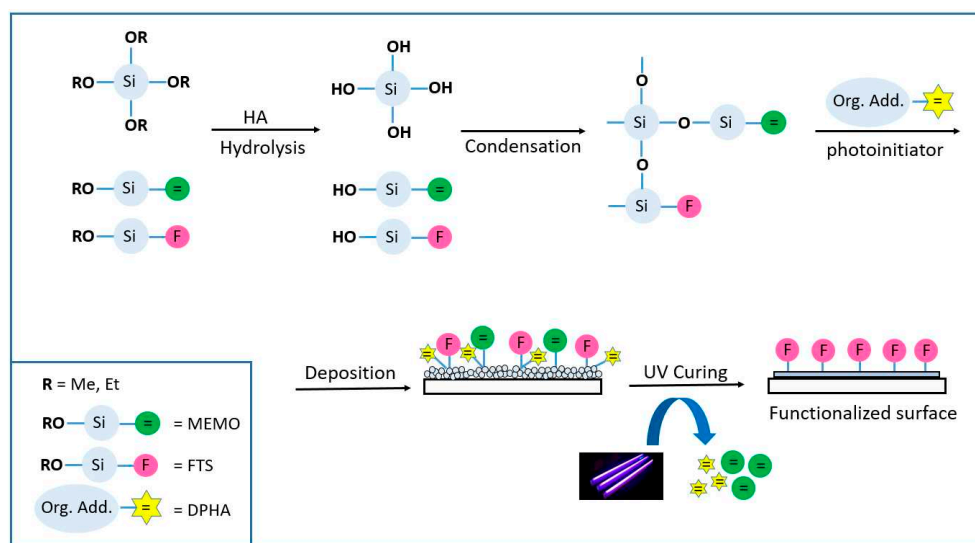

Figure 1. Fotocurable sol gel reaction scheme. Coating procedure.

Organic – inorganic hybrid sol gel coatings (OIH) were studied for their application over stainless steel [15] and other metal substrates, in order to evaluate corrosion protection [16]. Intermolecular interactions between the macromolecular existing structures and the metallic surface are reviewed in the literature to achieve low porosity, rigidity and adhesion to the metallic substrate, creating a good physical barrier against oxidation, corrosion and erosion among other processes.

A model of protective coating produced in five steps using mainly sol–gel methods was studied by Hughes et al. in the form of a multilayer coating system with a total thickness of about 16 μm [17]. They propose a protection with dual behavior: a protective barrier taking advantage of the OIH properties with a self-healing response. In this multilayer system, the formulation of the different layers is based on organic-inorganic hybrid sol gel matrix composition because of the advantage of being produced at room temperature conditions on an industrial scale, by using well-established and low-cost methods.

The first aim of this work is to analyze the levelling capability of a sol gel coating onto low-cost metallic substrates to prepare the material for an additional decorative PVD layer, which requires a smooth surface to be deposited. Although there are many studies in the literature based on levelling thermally cured sol gel coatings, to our knowledge, the UV curing version for this application has not been studied.

For example, Guillen et al. studied the levelling capability of sol gel SiO_2 layers onto titanium and Kovar (Fe54 Ni29 Co17) foil substrates [18]. In this work, the coatings were prepared by immersion techniques and the roughness of the coating was determined for different withdrawal rates, and therefore thickness of the film, after the dip-coating deposition method. The sintering step

of the sol-gel layers was obtained by heat treating in air at 400 °C for 1 h, and the Ra levelling parameter was improved (decreased) by adding successive sol gel SiO_2 layers with their corresponding heating treatment.

Similarly, it was recently described a method for the functionalization of low-cost steel with application on solar cells, with the properties of surface levelling, electrical insulation and anti-diffusion barrier [19]. The application method for this work was the spray coating and the samples were cured by near-infrared technique (NIR) at an irradiation power of 90%. A curing time of 2 min was applied in all cases (reaching a peak metal temperature of 198 °C), which represents a clear time reduction compared to conventional hot-plate curing (typically close to one hour).

In a thermal curing process, densification of the layer is usually obtained by heating at temperatures over 400°C. By using the fotocurable method, the levelling layer could be performed under mild processing conditions (low temperature and atmospheric pressure). For this purpose, AISI 430 stainless steel foils were covered with the optimal formulation parameters at various thicknesses, first by spin coating and later by spraying techniques, in a large-scale study. The analysis of the roughness, topography and morphology of these samples allowed us to conclude that a levelling functionality of the film has been achieved, with good adhesion properties and employing ultrafast curing methods.

On the other hand, we studied the addition of a fluoro-compound with a low surface energy in the appropriate step of the formulation to convert the previously designed coating onto a hydrophobic surface, thereby easily achieving a new functionality for different materials just by adding an extra additive. There are few examples in the literature for this kind of UV-curable coating [20,21] but all of them are focused exclusively on the coating of plastics such as polymethyl methacrylate or polycarbonate, and not applicable to metallic surfaces, requiring an extra step of heating before UV curing and applied by different methods in small samples.

Here we report the optimized formula for a dual-functional coating onto stainless steel surfaces, not only for laboratory scale but also for covering large areas and different geometries by employing different deposition methods.

2. Materials and Methods

2.1. Materials and chemicals

An AISI 430 stainless steel sheet with a thickness of 0.3 mm was cut into 50 x 50 mm^2 or 100x100 mm^2 sized substrates, depending on the scale up of the formulation and the application method studied. After cleaning with acetone, detergent and surfactant ultrasonically for 15 min, the samples were rinsed with distilled water and anhydrous ethanol and then dried with air. The AISI 430 chemical composition, analyzed by arc spark spectroscopy, is reported in Table 1.

Table 1. AISI 430 stainless steel composition.

Element	C	S	P	Si	Mn	Cr	Ni	Mo
Content	0.070	0.002	0.023	0.180	0.810	16,21	0.054	≤0.10

Concerning the sol formulation, tetraethyl orthosilicate (TEOS) for synthesis, 3-(Trimethoxysilyl) propyl methacrylate (MEMO, 98%) and the organic crosslinking agent, dipentaerythritol penta-/hexa-acrylate (DPHA) were purchased from Sigma-Aldrich. The photo-initiator, 2-hydroxy-2-methylpropiophenone (Darocure 1173) and the fluoroalkylsilane, triethoxy-1H, 1H, 2H, 2H-tridecafluoro-n-octyltriethoxysilane (F13), were purchased from TCI. Hydrochloric acid (37%, AnalaR® NORMAPUR® Reag. Ph. Eur. analytical reagent) and 2-propanol (≥99.7%, AnalaR NORMAPUR® ACS, Reag. Ph. Eur. analytical reagent) were purchased from VWR. All materials were used as received, except for 1H, 1H, 2H, 2H-Perfluorooctyltriethoxysilane (F13) which was transferred to an opaque two-necked flask and handled under nitrogen.

2.2. Synthetic procedure for the levelling layer

2.2.1. Laboratory scale

To prepare the sol-gel solution, 5 mL of TEOS were mixed with IPA in a molar ratio of TEOS/IPA=2.4 to form a homogeneous solution. Then, aqueous HCl (pH 1.2) was added under agitation to induce the sol-gel reaction with a H_2O/TEOS ratio of 4. The solution was stirred for 2 h at room temperature, after which MEMO (in a TEOS/MEMO ratio of 4.5), additional IPA (TEOS/IPA=6.4) and additional aqueous HCl (H_2O/MEMO= 3) were very slowly dropped into the formed silica sol. The reaction was continued for 2 h and appropriate amounts of DPHA and photo-initiator Darocure 1173 were added to the sol under vigorous agitation in TEOS/DPHA and TEOS/1173 ratios of 7.8 and 22.6, respectively, and stirred for 45. Finally, the sol was filtered and uniformly spread on 50 x 50 mm² AISI 430 stainless steel substrate samples by spin coating at 3000 rpm (rotation speed), followed by treatment under UVA irradiation (365 nm) with a conventional low-pressure mercury lamp with a power density of 0,2W/cm² for 15 minutes to yield a cured film.

2.2.2. Scale up for continuous coating

A re-optimization of the small scale process parameters was necessary to achieve the levelling functionality of the coating for the scale-up process, in order to obtain a homogenous coating free of cracks and ultrafast cured. In this procedure the water and the acid amounts were recalculated and added separately, but not scaled up in a linear mode. The reaction required the same amount of water to proceed but the catalyst charge was reduced to prevent the acid from attacking the surface of the metallic substrate when added in large quantities. Additionally, the photoinitiator was slightly reduced in quantity in this procedure, taking into account the rates of the curing step and the excess of the chemical added.

To prepare the sol-gel solution, 25 mL of TEOS (25 mL) were mixed with IPA in a (molar ratio of TEOS/IPA=2.4 to form a homogeneous solution. Then, H_2O in a H_2O/TEOS ratio of 3.7 and concentrated HCl 37% in a TEOS/ HCl ratio of 160 were added under agitation to induce the sol-gel reaction. . The solution was stirred for 2 h at room temperature, after which MEMO (in a TEOS/MEMO ratio of 4.2) and additional IPA (TEOS/IPA=6.9) were very slowly dropped into the formed silica sol. Additional H_2O (H_2O/TEOS = 0.6) and concentrated HCl 37% (TEOS/ HCl =430) were added under agitation. The reaction was continued for 2 h and appropriate amounts of DPHA and photo-initiator, Darocure 1173, were added into the sol under vigorous agitation in TEOS/DPHA and TEOS/1173 ratios of 7.8 and 21.5, respectively, and stirred for 45 minutes.

Finally, the sol was filtered, diluted to a 1:3 ratio in isopropanol, reaching a volume of approximately 150 mL and a viscosity of around 8-9 cP, and uniformly spread on 100 x 100 mm² AISI 430 stainless steel substrate samples using the spray method.

Spray coating was performed using a commercial air atomizing spray gun from Spraying Systems Inc., with a nozzle cone angle of 60°. The spray gun was mounted on an automatized spray system and moved transversely with respect to the sample movement. The 100 x 100 mm² samples were coated using the following parameters: (i) a sol–gel liquid pressure of 0.3 bar, (ii) an air pressure of 0.8 bar, (iii) a holder speed of 0.9 m/min, (iv) a nozzle/sample distance of 17 cm, and (v) a one scan spray. After deposition, samples were very fast cured under UV irradiation with a medium-pressure mercury lamp Light Hammer 10 (6,59W/cm²) equipped with a D-bulb, located in a specific coating pilot plant installed at our organization which allows for continuous coating in large areas. By setting a conveyor belt speed of 8 m/min and a distance of 200 mm between the light source and the samples, the curing step was performed in a flash mode of 1.5 seconds per sample.

2.3. Synthetic procedure for the hydrofobic/easy to clean coat

To prepare the sol-gel solucion, 5 mL of TEOS were mixed with IPA in a molar ratio of TEOS/IPA=2.4 to form a homogeneous solution. Then, aqueous HCl with a pH of 1.2 was added under agitation to induce the sol-gel reaction with a H_2O/TEOS ratio of 4. The solution was stirred

for 2 hours at room temperature, , after which MEMO (in a TEOS/MEMO ratio of 4.5), additional IPA (TEOS/IPA=6.4) and additional aqueous HCl (H2O/MEMO= 3) were very slowly dropped into the formed silica sol. The reaction was continued for 2 hours, and an appropriate amount of F13 was added with a F13/MEMO molar ratio of 1. The reaction was allowed to proceed for 1 hour, after which DPHA and photo-initiator Darocure 1173 were added to the sol under vigorous agitation in TEOS/DPHA and TEOS/1173 ratios of 7.8 and 22.6 respectively, and stirred for 45 minutes. Finally, the sol was filtered and uniformly spread on 50 x 50 mm² AISI 430 stainless steel substrate samples by spin coating at 3000 rpm, followed by treatment under UVA irradiation with a conventional low-pressure mercury lamp with a power density of 0,2W/cm² for 15 minutes to yield a cured film.

2.4. Characterization

The three-dimensional morphology and surface roughness of the samples were obtained using two different profilometers. A mechanical profilometer (Model XP-1, Ambios Technology, USA, with a resolution of 5 Å, perfile length of 1.25 mm and a cut-off of 0.25 mm), and an optical profilometer (WYCO-RST 500, using the vertical scanning interferometry (VSI) mode to measure the topography in an area of 0.9x1.5 mm). For each sample, readings were taken in at least three different positions and the average value was taken as the final value. The magnification of the surface was analyzed analyzed with an optical microscope (LEICA DMI5000M) to check for defects and surface integrity. The chemical composition of the sample surface was analyzed by an energy-dispersive X-ray spectrometer (EDS), while the chemical structure of the coating was analyzed by Fourier transform infrared spectroscopy (FTIR-ATR Nicolet 6700). The FTIR spectrum was obtained in the infrared region from 650 to 4000 cm^{-1} using a horizontal attenuated total reflectance device. All the spectra were recorded at 2 cm^{-1} resolution. Reflectance spectra were performed for the hybrid coating after UV curing. Thermogravimetric analysis (TGA) of the sol-gel solution and UV cured coatings was performed by using a TGA/DSC Mettler-Toledo thermogravimetric analyzer. The tests were run from 20 to 800 °C with a heating rate of 10 °C/min under an air atmosphere for the solution and under nitrogen for the UV-cured films. The static water contact angle was measured by a contact angle instrument (OCA 25, DataPhysics) using a droplet size of 1μL. The contact angles were obtained by averaging the measured values at four different locations on the inspected surface. The bonding strength between the coating and substrate was measured by the cross-hatch testing in accordance with ISO 2409:2020 standard. The hardness of the coatings was measured by nanoidentation employing a NanoIndenter XP (MTS) with a Berkovich diamond tip. The tip was calibrated on a fused silica sample using the Oliver and Pharr method [22]. The viscosity of the solutions was monitored using a Brookfield DVI-Prime viscosimeter. Physical vapor deposition (PVD) coatings were deposited in a commercial equipment (xPro4C PVT) equipped with four sputtering targets (700 x 105 mm). CrN and TiN coatings were deposited using HIPIMS technique at a controlled temperature of 80 °C.

3. Results and discussion

3.1. Levelling layer

The topography of the AISI 430 stainless steel substrate was studied before coating and a map obtained by optical profilometry is shown in Figure 2a. The average surface roughness (Ra) and the peak to valley roughness (Rt) of the uncovered substrate were determined by taking five different measurements along the surface, and the mean values were found to be 81 nm and 1.80 μm respectively.

Different samples (as shown in Table 2) were coated via spin coating at various rotation speeds (rpm) in order to change the thickness of the layer. In general, the higher the velocity of the spin coater, the thinner of the layer. The thickness was measured employing a mechanical profilometer. Additionally, the deposition of two consecutive layers was studied to analyze the effect on functionalization and to enhance the thickness in a different way by depositing a layer, UV curing, depositing the top coat and UV curing again. The average surface roughness (Ra) and the peak to

valley roughness (Rt) of these samples were also measured at five different points per sample (as shown in Figure 2b, c and d) to quantify the levelling functionality of the sol-gel coating and the influence of the thickness on the levelling effect.

Table 2. Thickness and roughness of samples covered at different conditions.

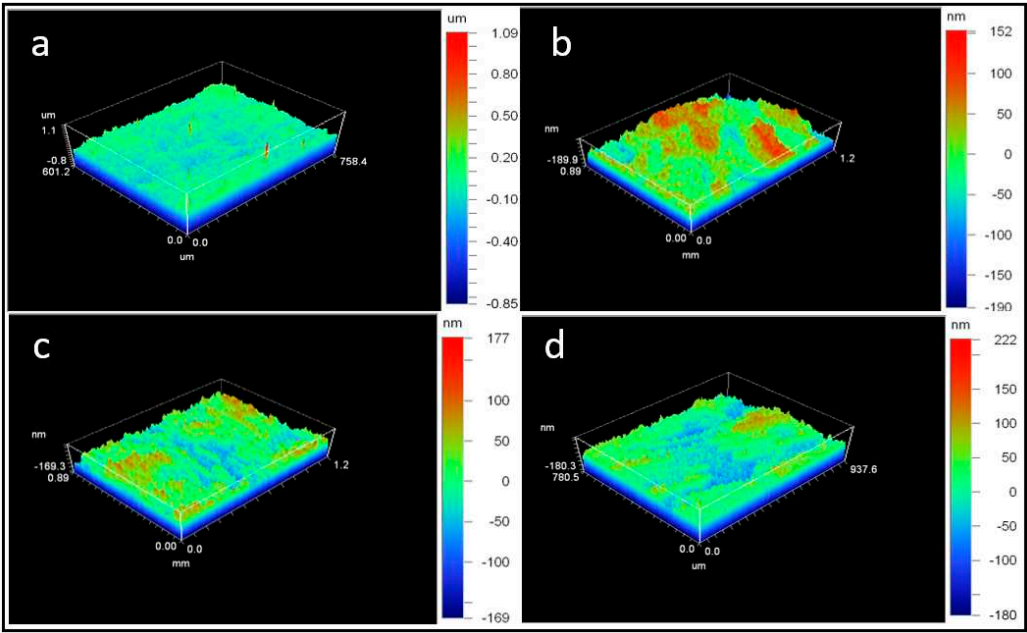| Entry	Sample	rpm 1st layer	rpm 2nd layer	Coat thickness (μm)	Ra (nm)	Rt (μm)
1	AISI 430	-	-	-	81	1.80
2	A	500	-	6.7	20	0.14
3	B	1000	3000	7.3	27	0.19
4	C	2000	3000	5.7	29	0.21
5	D	3000	-	1.7	23	0.17

Figure 2. 3D images obtained through optical profilometry of the surface of the studied samples: (a) AISI430SS; (b) Sample A; (c) Sample B; (d) Sample C.

The deposition of the sol-gel coating on AISI 430 stainless was designed to act as a levelling layer, independent of the thickness of the coating and the number of layers deposited (as shown in entries 2 – 5 in Table 2). In fact, the average surface roughness (Ra) of these samples was reduced to one-quarter of their value in the uncoated substrate, and the peak to valley roughness (Rt) decreased to around 200 nm compared to the uncoated substrate, where this value was 1800 nm (as shown in entry 1). It was also shown that it was possible to achieve various thicknesses of the coating, by slowing down the spinning of the coater or by introducing multiple layers on top, regardless of maintaining the levelling functionality intact. The surface did not present visible defects and uniformity was observed when sample D (entry 5) was analyzed with an optical microscope (as shown in Figure 3).
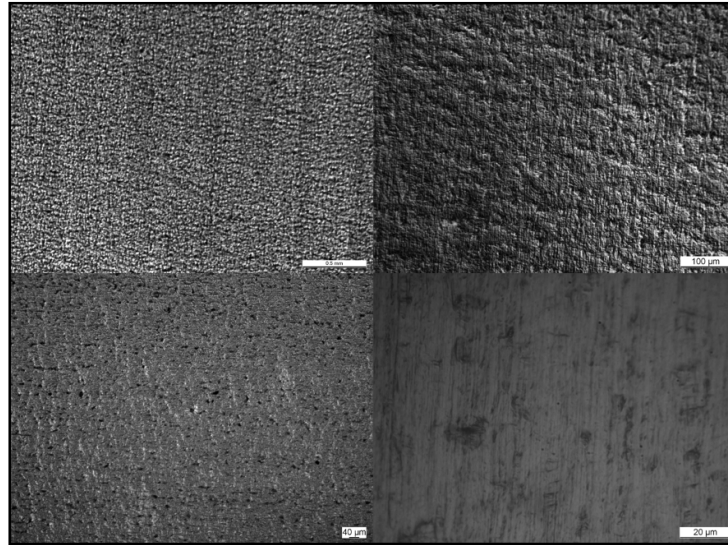
7

Figure 3. Magnification of the surface of AISI430SS covered with a 1.7 μm-thick SiO_2 layer to the microscale.

- Adhesion test

A good adhesion to the substrate and mechanical properties of the coating are critical points to meet the surface properties required [23]. In order to guarantee the adherence and permanence of the coating, an adhesion test (cross cut test) was performed on a sample coated with the sol-gel studied in accordance with ISO 2409:2020 standard. The test involved making six vertical and six horizontal cuts, forming squares of 1 mm × 1mm. An adhesive tape was applied and then removed from the cut area of the coated sample. Some pictures of the tested area were taken with an optical microscope (as shown in Figure 4), which showed that the substrate AISI 430 was exposed in the area where the coating was removed. It was observed that the coating pulled out only in the region of the incision, without causing damages to the rest of the film. This result indicates that the sol-gel layer exhibited strong adherence to the substrate, which is an essential factor to guarantee a long service life of the final product.
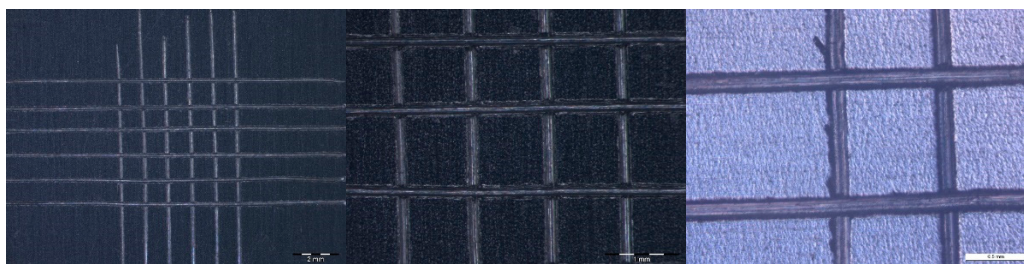

Figure 4. Magnification of the surface and cuts of AISI430SS covered with a 1.7 μm-thick SiO_2 layer after the adherence test performed.

- Hardness

In these type of coatings, hardness is usually quantified as pencil hardness since they are more flexible and soft coatings than the thermally cured ones. Although only planar samples were coated in this study, these features allow the coating of many different geometries without disrupting the layer integrity. Nevertheless, a pencil hardness of 6H is considered hard. The hardness of the cured films in this work was examined by pencil test, giving a result of 9H, which is the maximum value, in which the coating could not be torn off the substrate. Hardness was also examined by nanoindentation [24] in order to determine the coating's mechanical characteristics and to compare with other coatings in the literature. In this approach, a defined indenter tip is forced into a specified spot in the test sample, and gradual unloading is conducted until the required depth is achieved. The

analysis was performed in four equivalent samples with similar coating thickness, and two different forces of 500 and 1000 µN were applied (higher forces were too deep in the coating for a reliable measurement). When 1000 µN were applied, the values of hardness and Young modulus were slightly higher, indicating that the proximity of the substrate was influencing the measurement at some level. The results are gathered in Table 3, showing good repeatability, which translates to good homogeneity of the layer. The values of hardness around 0.3 GPa indicate the typical low hardness of these films, and the elastic modulus showed quite good elasticity when compared with coatings cured under thermal conditions.

Table 3. Hardness results of coated samples acquired by nanoindentation.

Sample[1]	Thickness	Force	H± σ (GPa)	E± σ (GPa)	δ_c (nm)
E	1.9±0.1	500µN	0.332±0.006	5.15±0.08	214
F	1.6±0.2	500µN	0.392±0.016	5.42±0.16	192
G	1.6±0.2	500µN	0.332±0.007	5.15±0.09	213
H	1.6±0.1	500µN	0.306±0.006	4.26±0.10	225
I	1.9±0.1	1000 µN	0.372±0.006	6.73±0.13	305
J	1.6±0.2	1000 µN	0.394±0.019	6.37±0.15	295
K	1.6±0.2	1000 µN	0.370±0.009	6.65±0.09	306
L	1.6±0.1	1000 µN	0.339±0.005	4.77±0.06	322

[1] A total of 25 indentations were done per sample at the two different forces.

To demonstrate the feasibility of the method for coating different geometries, thanks to the good elasticity of the coating, a stainless steel cylinder was coated using the spray coating technique (as shown in Figure 5) after following the procedure described in section 2.2.2. For this purpose, an automated robotic spray coating system (Fisnar F4400N) was employed. The best conditions were studied to achieve a uniform and continuous coating with a thickness of around 6 µm over the entire surface. The following parameters, after diluting the solution to 1:2 with isopropanol were set as the optimized ones: (i) a sol–gel liquid pressure of 0.5 bar, (ii) an air pressure of 1.2 bar, (iii) a nozzle coating speed of 3 mm/s and (iv) a nozzle/sample distance of 7 cm. After deposition, the piece was cured by spinning over a platform and exposed to UVA irradiation with a low-pressure mercury lamp for 30 minutes. Additionally, the application of consecutive layers of the coating was studied, and a thickness of 20 µm could be reached, by depositing three consecutive layers while applying the parameters described above.
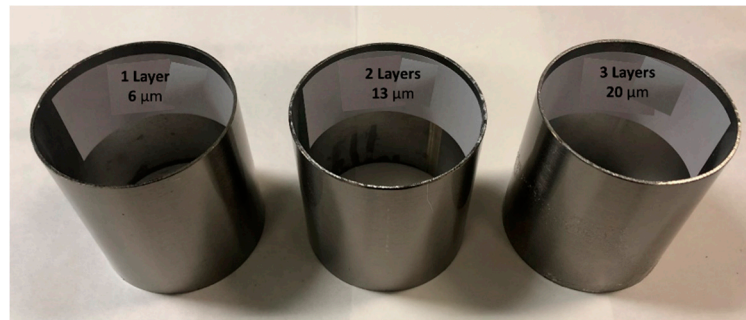
Figure 5. Stainless steel cylinder coated with the sol gel formulation using a robotic spray coating system, and thickness of the coating after deposition of multiple layers.

- Aging study of the sol

Despite the promising properties of the sol–gel layer there are certain important challenges that need to be overcome before wide industrial applications can be considered. One decisive factor in determining the composition, functionality and integrity of the final coating is the period between solution preparation and coating deposition.

During the sol–gel synthesis the hydrolysis of alkoxides occurs in the presence of water and partially hydrolyzed precursors are formed along with condensation reactions. During the post-synthesis aging, these chemical reactions are not stopped in the system and continue propagating, following the condensation step in which partially hydrolyzed precursors are polymerized, depleting the amount of available silanol groups. The long-term aging effects usually cause destabilization of the sol–gel due to the extended progress of condensation reactions, and often even gelation of the formulation before it is applied to a substrate. The intensity of gelation can be quantified by measurement of the viscosity of the solution. Usually an increase of the viscosity can affect the thickness of the layer, and it is possible to reach a critical thickness beyond which the coating losses its integrity and a partial degradation of the functionality.

In real industrial practice, long storage times are often required. In order to guarantee a long service life of the solution before deposition over large areas, the formulation was scaled up (as specified in section 2.2.2) and monitored with respect to the viscosity before deposition, so that the thickness and roughness parameters could be measured after deposition over the substrate. The data obtained is detailed in Table 4, and a graphical monitoring is represented in Figure 6. The solution was stored in the dark during the test to prevent possible curing under visible light.

Table 4. Monitoring of different parameters while storage before and after deposition.

Time (h)	Viscosity (Cp)	Thickness (µm)	Ra	Rt
1	15.4	2.9	28	180
3	15.4	2.6	29	220
19	16.0	2.7	30	229
24	16.0	2.6	24	173
48	15.8	2.9	30	187
192	17.5	3.0	30	192
216	18.0	3.1	28	190
240	17.8	2.8	36	252
264	19.4	3.5	45	301
336	19.4	3.7	47	320

As can be observed from the analysis of the samples and acquisition of the corresponding data, viscosity and thickness increased suddenly after 240 hours of storage. Before this time, a thickness of approximately 3 µm is maintained, with a coating layer that does not present any defect or crack, thus preserving the desired functionality. Additionally, the Ra and Rt values start to increase at this time, with Ra being > 30 nm and Rt being > 300 nm (values considered optimal for the levelling effect). The increase in these parameters can be observed in Figure 6, although the increment is quite slow.
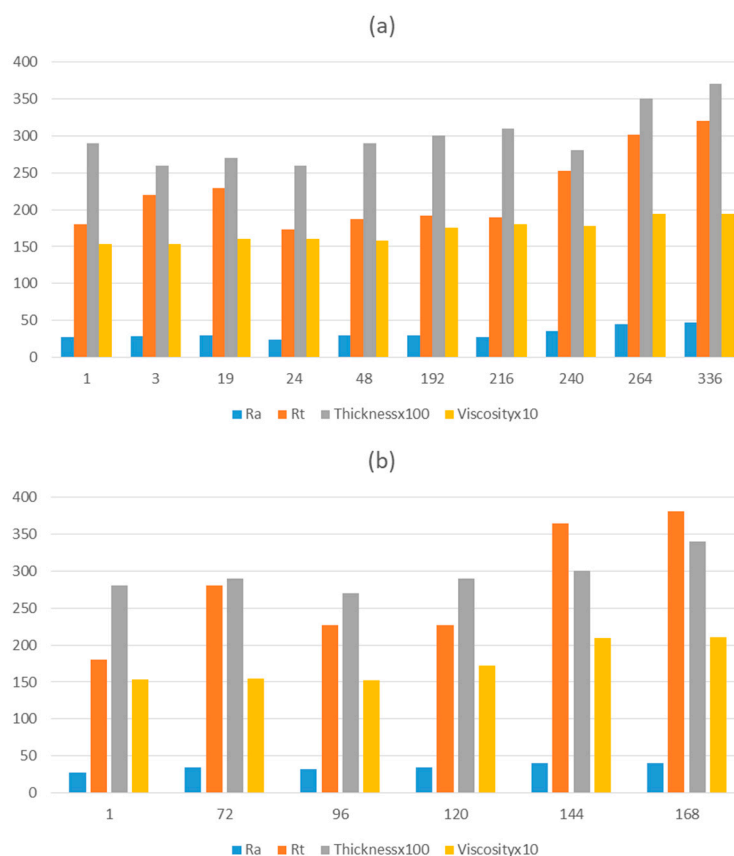

Figure 6. Progress of various parameters over time before and after deposition of the levelling sol-gel coating for determination of the service life: (a) in the dark, and (b) exposed to light.

The aging stability and corresponding shelf-life of the solution, focused on an industrial application, could be determined through this study, establishing a period of 240 hours (10 days) during which the formulation (stored in the dark) is in optimal conditions to be applied over the substrate. The same study was conducted for the storage under light (as shown in Figure 6(b), and a maximum of 120 hours (5 days) was determined to guarantee the properties of the coating. Beyond 120 hours, viscosity increases, affecting the total roughness, with values of Rt > 300 nm being outside the desired range. Therefore, the functionality of the coating cannot be guaranteed for longer storage periods.

3.2. Easy to clean layer

The main objective of this part of the work was to modify the sol-gel coating formulation by fluorination to obtain hydrophobic surfaces with low surface energy, which have interesting applications in the domestic sector, where self-cleaning ability is often required for many materials.

It is important to take into account that, usually, roughness enhances hydrophobicity depending on the nature of the corresponding flat surface [25].Therefore, in this work, the smooth topography of the surface is playing a negative role in achieving the objective of enhancing hydrophobicity through fluorination.

In order to achieve hydrophobicity functionality of the coating, different fluoroalkyl compounds were studied by adding certain amount in the appropriate step of the formulation process, just before the organic partner DPHA. These organic groups replace the Hs of the surface OHs of the silica films during the sol–gel process forming a layer on the surface which is non-hydrolyzable and hence hydrophobic.

When a fluoroalcoxysilane is employed, such as 3,3,3-Trifluoropropyl-trimethoxysilane or Triethoxy-1H, 1H, 2H, 2H-heptadecafluorodecylsilane (F3 and F17 respectively in Figure 7), they interconnect with the polysiloxane network, and the contact angle on the surface is increased to 77 and 105° respectively, making the surface hydrophobic. In the case of employing a different agent with a fluorinated backbone but without silyl ether groups like 2H, 3H-Decafluoropentane (F10 in Figure 7), the effect obtained is the opposite, as the WCA observed is only 34°, making the surface more hydrophilic than the untreated one (No F in Figure 7). The best result was found when F13 (1H, 1H, 2H, 2H-Perfluorooctyltriethoxysilane) was employed as the hydrophobicity agent, where the WCA could be incremented to 113° and the water droplet adopts a more spherical shape. The molar ratio of F13/MEMO = 1 was optimized to achieve the best result, as it was observed that even doubling the quantity of the chemical lead to poorer contact angles (F13x2 in Figure 7).
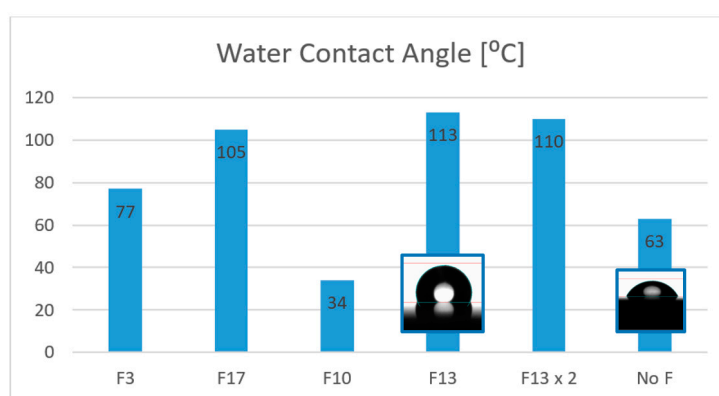

Figure 7. Water contact angles of UV curing sol gel coatings on AISI 430 by addition of different fluorinated compounds including photographs of the water droplet of the more representative results.

To test the self-cleaning ability of the coated surface, a more visual experiment was performed and documented by photographs taken with the goniometer. Figure 8 shows the testing process of dust removal by water droplets. The dust was absorbed by the water droplet and collected from the surface, confirming the anti-sticking property of the coating. With a contact angle hysteresis of 40° and by increasing the volume of the droplet [26], it rolls and slides on the inclined hydrophobic surface. It is possible to observe how the water picks up dust particles from the hydrophobic surface, dragging them by sliding down the material.
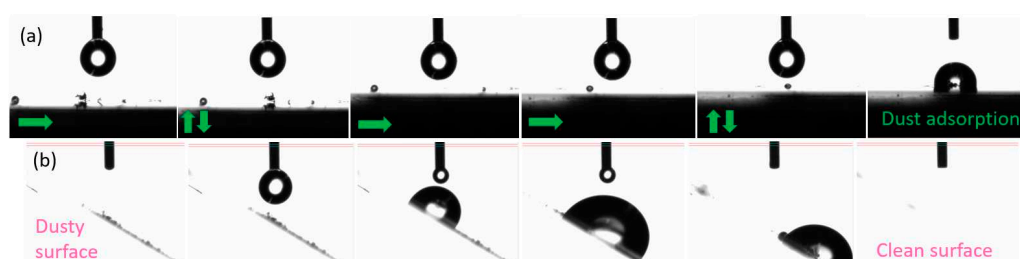

Figure 8. Process of dust absorption test by a water droplet on (**a**) planar hydrophobic surface (arrows indicating the platform moving direction); (**b**) hydrophobic surface at an angle of 40° and consequent sliding of the droplet (when increasing volume) dragging dust.

Furthermore, in order to study the application of the coating for domestic pieces resistant to the abrasion of cleaning products, a hydrophobic top coat was deposited onto a multilayer system consisting of an AISI substrate treated with a sol gel levelling layer and coated by PVD with TiN (gold finish) or CrN (silver finish). The multilayer example is represented in Figure 9.

Figure 9. Schematic drawing of the multilayer system and pictures of the gold and silver finish reached under the top coat.

In order to analyze the effects on the different layers, roughness and WCA were measured after deposition of each coating, and the results are collected in Table 5, as the average of measurements taken at three points over the surface. Several conclusions can be drown from the acquired data: (i) the first sol-gel layer works as a levelling coating, reducing the roughness of the AISI430 substrate to the expected objective (Ra < 30 nm and Rt < 300 nm) and while the surface remains hydrophilic (WCA < 90 °); (ii) the silver finish by PVD coating can be deposited over the levelled sol-gel surface through the HIPIMS method, resulting in a significant increase in roughness and, unexpectedly, an intrinsic hydrophobicity (which is transitory and is lost over the time) (iii) the protective sol-gel topcoat leads to a durable hydrophobic layer which also works as leveling layer, reducing Ra and Rt to the same values as the first layer.

Table 5. Monitoring of roughness and WCA for the different coatings of the multilayer system.

Layer	Ra (nm)	Rt (nm)	WCA (°)
AISI430 untreated	81	1800	88
Leveling SG	28	190	63
PVD Cr-N	39	1191	90-105
Protector SG	17	195	113

- UV irradiation test. Transparency

The coated samples were tested against UV irradiation to determine whether there were color changes and to ensure that there were no alterations of the visual aspect after long periods of time, as well as to assess the durability of hydrophobic/protector functionality. The UV irradiation tests of the films were conducted using a QUV-weathering tester (QUV/Solar Eye Spray). The samples were exposed to UVA irradiation (340 nm) with a power of 0. 76 W/m² at 45 °C for 300 hours, and the WCA of the samples was measured at different UV irradiation times.

Color data were measured before (sample M in Table 6) and after (samples N-P in Table 6) UV irradiation for different periods of time using a BYK-Gardner spectro-guide sphere color spectrophotometer. The coordinates of color of samples M, N, O and P, as well as their ΔE values calculated from Equation 1 before and after solar irradiation are listed in Table 4. ΔE values were calculated using the color data, where L* is the level of light or dark, a* means redness or greenness and b* is the coordinate that indicates yellowness or blueness.

$$E = \sqrt{[(L_a - L_b)^2 + (a_a - a_b)^2 + (b_a - b_b)^2]} \qquad (1)$$

The ΔE value was measured throughout time of exposure, and de total ΔE value is expressed in Table 6, which measures the difference of color between sample M and sample P, after 300 hours under UV radiation. Based on the reviewed bibliography, a ΔE value of less than 3 indicates that the change in color cannot be perceived by the naked eye [27,28]. Therefore, no distinguishable color difference was observed in the covered AISI430 surfaces obtained in the scope of this study. The coating studied does not alter the visual aspect of the substrate, and the human eye cannot notice the color change even after long UV exposure times. This makes the coating potentially applicable as a decorative protector film for the domestic sector.

The protector functionality against cleaning products is unaltered after the light exposure, as can be verified by the measurement of the water contact angle with a water droplet (which does not change after the aging cycles, as shown in Table 6).

Table 6. Coordinates of color and ΔE values for samples exposed to UV radiation test.

Sample	Time (h)	WCA(°)	L*	a*	b*	ΔE	ΔE tot
M	0	113.3	68,26	0.32	2,21	-	-
N	72	113.4	67,70	0.88	2,92	1,06362587	-
O	150	113.6	69,01	0.21	3,24	1,50578883	-
P	300	113.2	67,92	0.33	3,95	1,30636901	1,77293542

3.3. Chemical analysis of the coatings

- Thermogravimetric Analysis (TGA)

The thermal properties of the hybrid films were evaluated with the TGA analysis to ensure the thermal resistance of the coatings once cured. The thermo-gravimetric analysis was also performed on the uncured sol gel solution for the levelling formulation to compare differences. When examining the TGA thermogram for the levelling hybrid sol-gel solution (represented in blue color in Figure 10) thermal decomposition follows a two-stage process at 106 °C and 462 °C, with 12% and 47% weight loss respectively. The TGA analysis for the corresponding cured hybrid film (represented in red in Figure 10) shows a thermal decomposition process following two stages at 66 °C and 442 °C, respectively. The data collected indicated that there was only a 4% loss of weight in the range of 0–140 °C, due to the evaporation of residual solvents or moisture trapped in the film, which were eliminated at the beginning of the heating treatment. The 51. 7% loss of weight was observed at approximately 442 °C, which is similar to the not sintered coating.

In the case of the protector sol-gel cured coating (represented in black in Figure 10), thermal decomposition follows a four step pattern in which the loss of weight observed at 57 and 190 °C is a total of 7% loss, assignable to the solvent or volatile compounds evaporation. The maximum loss of weight at 421 °C was 32% loss. Moreover, the DTA thermogram for this film indicates a new decomposition stage around 491 °C (16% loss of weight), which may be associated with the decomposition of sol–gel precursor content F13. The char yields at 800 °C were also collected for all the formulations, showing a 41% residue in the solution levelling formulation, 44% in the cured one, and 34% for the protector sol-gel coating.
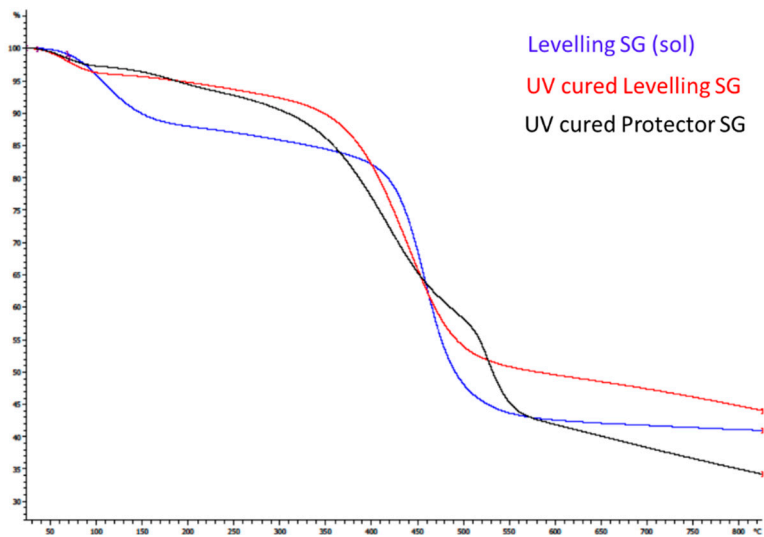
Figure 10. Thermogravimetric analysis (TGA) thermogram for levelling sol gel coating solution (blue), the UV-cured levelling coating (red) and the UV-cured protector hybrid film (black).

This analysis confirms that both formulations are thermally resistant at temperatures up to 350 °C, which is a considerable high resistance for a hybrid sol-gel coating cured under UV light.

- Fourier-transform infrared spectroscopy (FTIR)

The FTIR spectrum of the sol-gel coating solutions for the levelling and protector functionalities are represented in Figure 11. Both of them show the typical signals for this kind of organic-inorganic hybrid coatings, with the difference being the presence of fluoro-alkylated chain peaks, which are only observed in the protector coating confirming that the formulation is identical, with the only difference being the addition of this substance. The assignment of the signals is collected in Table 7.

Some of the common absorption bands of a sol-gel coating were found at 1045 cm^{-1} which correspond to the stretching vibrations of Si-O-Si bonds, at 948 cm^{-1} which is assigned to the Si-OH groups formed from hydrolysis of TEOS and the broad band around 3340 cm^{-1} which stands for the asymmetric stretching of various of these OH groups and others coming from moisture, residual solvent, etc. The asymmetric C–H stretching peaks for the methyl groups are located at 2970 cm^{-1} and 2890 cm^{-1}, with the later also being a signal for the C–H stretching peak of the methylene group present in the molecular formula of MEMO and DPHA. The other clearest peak, is the stretching vibration peak for the carbonyl group that was observed at a wavelength of around 1715 cm^{-1} in both formulations. This signal and the one found at 1635 cm^{-1}, corresponding to a C=C bond stretching, are assignable to the chemical formula of MEMO. The decreasing of this signal is usually observed in hybrid sol-gel coatings when the curing step takes place, as the C=C of the MEMO reacts with the hexa-functional monomer DPHA, which can polymerize to form a cross-linked network via a photo-sensitive UV-curing process. Nevertheless, this peak does not disappear after curing in our case, presumably due to an excess of MEMO in the formulation.

The signals associated with 13F can be found in the protector sol-gel spectrum at 1240 and 695 cm^{-1} corresponding to the Si-CF$_3$ and C-F bond stretching, respectively. Other characteristic peaks of 13F are not in evidence because of overlapping with those of MEMO.

Table 7. FT-IR wavenumbers and observed signals of the SG coating solutions.

Assignments	Peak wavenumber (cm^{-1}) Levelling SG	Peak wavenumber (cm^{-1}) Protector SG
-OH	3342,2	3331,0
-CH$_3$	2972,9	2973,5
-CH$_3$, -CH$_2$	2895,3	2891,8
-C=O	1716,7	1714,1

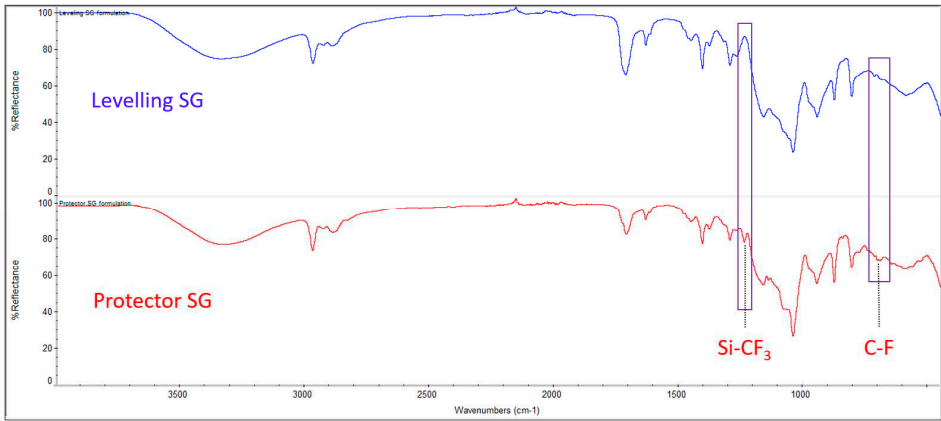| -C=C | 1635,3 | 1635,7 |
-Si-CF$_3$	-	1240,0
-Si-O-Si	1044,6	1045,1
-Si-OH	948,7	949,8
-C-F	-	695,6

Figure 11. Fourier-transform infrared spectroscopy (FTIR) spectrum for the coating solutions designed for levelling and protector hybrid films.

- Energy dispersive X-ray spectroscopy (EDS)

The composition of the surface of the two different coatings was also analyzed by EDS by using the scanning electron microscope (SEM) equipment at 20 kV. The data is presented in Table 8 and represented in Figure 12. The composition was measured as weight and atomic percentage, and only C, O and Si were detected along the area selected, as expected. It was also found that the weight content of fluoride is 20 % for the protective coating and inexistent for the levelling formulation, and the quantities of elements C and Si remain unaltered.

Table 8. Weight % and atomic % elemental composition by EDS of both coatings.

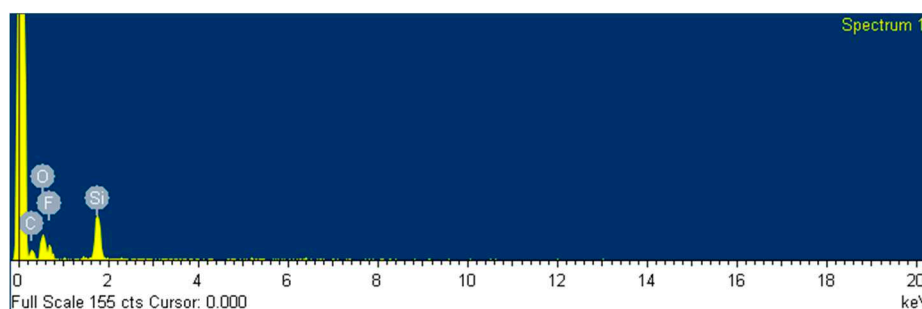|	Weight %				Atomic %			
Element	C	O	F	Si	C	O	F	Si
Levelling SG	24,05	55,04	0,00	20,91	32,36	55,61	0,00	12,03
Protector SG	23,93	35,67	19,58	20,82	33,24	37,20	17,19	12,37
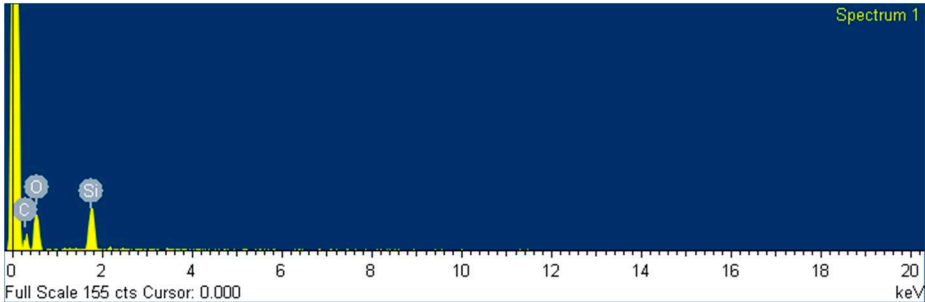
Figure 12. EDS analysis for the levelling sol gel coating (top) and the protector sol gel coating (bottom).

5. Conclusions

This scalable and low cost technique for coating stainless steel provides an optimum protective and levelling barrier suitable for many industrial applications. Moreover, a multilayer system was performed to demonstrate the suitability of the method for applying consecutive coatings of different materials, deposited by sol-gel and PVD, for use in components in the domestic sector.

While hybrid organic-inorganic coatings have been studied before, there are no many examples in the literature showing this dual effect simply by adding an extra additive. Instead of deposition over a polymer, the functionality pursued was studied over AISI430 as an alternative method for coating in an ultrafast mode without the use of high temperatures that could affect the internal layers of the system. In addition, the intrinsic flexibility of this type of hybrid coatings allows for the functionalization of components with different geometries, not restricted to planar samples.

A full characterization of the layers is included, showing good adherence to the substrate, considerable hardness and thermal resistance, as well as accomplishing the functionality pursued in each case. The method is scalable with a simple re-optimization of the parameters and applicable to large areas using the spray coating method. An aging study of the formulation also allows for the guarantee of the solution's shelf-life before deposition, opening the door to a possible industrialization method of functionalizing stainless steels for many interesting applications.

Supplementary Materials: Not applicable.

Author Contributions: Conceptualization, L.F and R.B.; methodology, L.F.; analysis, L.F., J.M. and J.F.; investigation, L.F.; writing—original draft preparation, L.F.; writing—review and editing, L.F.; supervision, O.C. and R.B.; project administration, O.C.; funding acquisition, R.B. All authors have read and agreed to the published version of the manuscript.

Institutional Review Board Statement: Not applicable.

Informed Consent Statement: Not applicable.

Data Availability Statement: Not applicable.

Conflicts of Interest: The authors declare no conflict of interest.

References

1. Livage, J. Sol-Gel Synthesis of Inorganic Materials. In Encyclopedia of Materials: Science and Technology; Buschow, K.H.J., Cahn, R.W., Flemings, M.C., Ilschner, B., Kramer, E.J., Mahajan, S., Veyssière, P.B., Eds.; Elsevier: Oxford, UK, 2001; pp. 4105–4107. ISBN 978-0-08-043152-9.
2. Handbook of sol-gel science and technology: Processing, characterization, and applications. Choice Rev. Online 2013.
3. Kordas, G. Sol-gel processing of ceramic superconductors. J. Non.-Cryst. Solids 1990, 121, 436–442.

4. Vincenzini, P. High Performance Ceramic Films and Coatings; North-Holland Publishing, Co.: Amsterdam, The Netherlands, 1991; ISBN 978-0444890580.

5. Kim, H.K.; Kang, S.-J.; Choi, S.-K.; Min, Y.-H.; Yoon, C.-S. Highly Efficient Organic/Inorganic Hybrid Nonlinear Optic Materials via Sol-Gel Process: Synthesis, Optical Properties, and Photobleaching for Channel Waveguides. Chem. Mater. 1999, 11, 779–788.

6. Owens, G.J.; Singh, R.K.; Foroutan, F.; Alqaysi, M.; Han, C.-M.; Mahapatra, C.; Kim, H.-W.; Knowles, J.C. Sol-gel based materials for biomedical applications. Prog. Mater. Sci. 2016, 77, 1–79.

7. Avnir, D.; Braun, S.; Lev, O.; Ottolenghi, M. Enzymes and Other Proteins Entrapped in Sol-Gel Materials. Chem. Mater. 1994, 6, 1605–1614.

8. Inayat, A.; Reinhardt, B.; Herwig, J.; Küster, C.; Uhlig, H.; Krenkel, S.; Raedlein, E.; Enke, D. Recent advances in the synthesis of hierarchically porous silica materials on the basis of porous glasses. New J. Chem. 2016, 40, 4095–4114.

9. Feinle, A.; Elsaesser, M.S.; Hüsing, N. Sol-gel synthesis of monolithic materials with hierarchical porosity. Chem. Soc. Rev. 2016, 45, 3377–3399.

10. A P Periyasamy, M. Venkataraman, D Kremenakova, J. Militky and Y Zhou. Progress in Sol-Gel Technology for the Coatings of Fabrics. Materials 2020, 13, 1838.

11. A. Bifulco, C. Imparato, A. Aronne and G. Malucelli. Flame retarded polymer systems based on the sol-gel approach: recent advances and future perspectives. Journal of Sol-Gel Science and Technology, 2022, https://doi.org/10.1007/s10971-022-05918-6.

12. A. Rosenhahn et al. Sol−Gel-Based Hybrid Materials as Antifouling and Fouling-Release Coatings for Marine Applications. ACS Appl. Mater. Interfaces, 2020, 12, 47, 53286–53296.

13. Shukla, V., Bajpai, M., Singh, D.K., Singh, M. and Shukla, R. Review of basic chemistry of UV-curing technology. Pigment & Resin Technology 2004, Vol. 33, pp. 272-279.

14. Yusuf Y., Steffen J., and Nicholas J. T. Photoinitiated Polymerization: Advances, Challenges, and Opportunities. *Macromolecules* **2010**, *Vol. 43*, 6245–6260.

15. V.H.V. Sarmento, M.G. Schiavetto, P. Hammer, A.V. Benedetti, C.S. Fugivara, P.H. Suegama, S.H. Pulcinelli and C.V. Santilli. Corrosion protection of stainless steel by polysiloxane hybrid coatings prepared using the sol–gel process. Surface & Coatings Technology 2010, 204, 2689–2701.

16. R. B. Figueira, C. J. R. Silva, E. V. Pereira, Organic–inorganic hybrid sol–gel coatings for metal corrosion protection: a review of recent progress. J. Coat. Technol. Res. 2014 DOI 10.1007/s11998-014-9595-6.

17. AE. Hughes, IS. Cole, TH. Muster, RJ. Varley, Designing Green, Self-healing Coatings for Metal Protection. NPG Asia Mater., 2010, 2, 143–151.

18. C. Guillén et al. Leveling effect of solgel SiO2 coatings onto metallic foil substrates. Surface and Coatings Technology 2001, 138, 205-210.

19. M.F Menendez, A. Martinez, P. Sanchez, D. Gomez, L.J. Andres, L. Haponow, N. Bristow, J. Kettle, T. Korochkina and D.T. Gethin. Development of intermediate layer systems for direct deposition of thin film solar cells onto low cost steel substrates. Solar Energy 2020, 208, 738–746.

20. Ömer Kesmez. Preparation of UV-curable hybrid films via sol–gel synthesis for hydrophobic surface applications. Journal of Sol-Gel Science and Technology. 2019, 91, 1–10.

21. C. Chang, Z. Lin, S. Huang and L. Cheng. Preparation of Highly Transparent 13F-Modified Nano-Silica/Polymer Hydrophobic Hard Coatings on Plastic Substrates. Journal of Applied Science and Engineering, 2015, 18, No. 4, 387-394.

22. W. Oliver, G. Pharr. Measurement of hardness and elastic modulus by instrumented indentation: Advances in understanding and refinements to methodology. J. Mater. Res. 2004, 19 (1), 3–20.

23. J. Z. Ferreira et al. Obtainment and Characterization of a Silicon alkoxides-based Coating Applied to a Substrate of Stainless Steel 316L for Use in Biomaterials. Materials Research, 2019; 22(3): e20180514.

24. A. E. Langroudi. A Brief Review of Nanoindentation Technique and its Applications in Hybrid Nanocomposite Coatings. Int. J. Bio-Inorg. Hybd. Nanomat., 2013, 2(2), 337-344.

25. L. Hyuneui, J. Dae-Hwan, N. Jung-Hyun, C. Gyeong-Rin, K. Wan-Doo. Fog Deposition and Accumulation on Smooth and Textured Hydrophobic Surfaces. Chin. Sci. Bull. 2009, 54, 3613.

26. G. Abdelmagid,B. S. Yilbas, A. Al-Sharafi, H. Al-Qahtania and N. Al-Aqeelia. Water droplet on inclined dusty hydrophobic surface: influence of droplet volume on environmental dust particles removal. RSC Adv., 2019, 9, 3582.

27. CIE. Technical Report: Colorimetry. CIE Pub. Nº 15.3 CIE Central Bureau, Viena, Austria, 2004.

28. Ö. Kesmez, E. Akarsu. Corrosion-resistant hybrid coatings for copper surfaces substrates by sol–gel chemistry. J Turkish Chem. Soc. Sect. 2017, A 4:1.